7. Lockhart, R. W., and R. C. Martinelli, *Chem. Eng. Progr.*, **45**, No. 1, pp. 39-48 (1949).
8. Linning, D. L., Ph.D. thesis, University of Glasgow, Glasgow, Scotland (1951).
9. Charvonia, D. A., *Armed Services Technical Information Agency Document AD-208,040, Project Squid Tech. Rept. PUR-32-R* (December, 1958).
10. Jens, W. H., and G. Leppert, *J. Am. Soc. Naval Engrs.*, **67**, 137, 437 (1955).
11. Rodabaugh, Rowena, *Two-Phase Flow and Acoustic Phenomena in Gases and Liquids: Literature Search No. 177*, Jet Propulsion Laboratory, California Institute of Technology, Pasadena, California (June, 1960).
12. Pike, R. W., Ph.D. thesis, Georgia Inst. Technol., Atlanta, Georgia (1962).
13. Kuntz, K. S., "Numerical Analysis," Chap. 7, McGraw-Hill, New York (1957).
14. "A Reference Manual: Burroughs Algebraic Compiler," Burroughs Corporation, Detroit, Michigan.
15. Keenan, J. H., and F. G. Keyes, "Thermodynamic Properties of Steam," Wiley, New York (1956).
16. Pike, R. W., Ph.D. thesis, p. 39, Georgia Inst. Technol., Atlanta, Georgia (1962).
17. *Ibid.*, p. 60.
18. Hatch, M. R., and R. B. Jacobs, *A.I.Ch.E. Journal*, **8**, No. 1, pp. 18-25 (1962).
19. Houghton, Gerald, *Nuclear Sci. and Eng.*, **12**, 390-397 (1962).
20. Anderson, G. H., G. G. Haselden, and B. G. Mantzouranis, *Chem. Eng. Sci.*, **16**, 222-230 (1961).
21. Bottomley, W. T., *Trans. North East Coast Inst. Engrs. and Shipbuilders*, **53**, 65-100 (1936-1937).
22. Burnell, J. G., *Eng.*, **164**, 752 (1947).
23. Linning, D. L., Ph.D. thesis, p. 207, Univ. Glasgow, Glasgow, Scotland (1951).
24. Isbin, H. S., J. E. Moy, and A. J. R. Da Cruz, *A.I.Ch.E. Journal*, **3**, 361 (1957).
25. Faletti, D. W., and R. W. Moulton, *ibid.*, **9**, 247-253 (1963).
26. Zaloudek, F. R., *HW-68934* (March, 1961).
27. Fauske, H. K., *ANL-6633* (Oct., 1962).
28. Tek, M. R., "Handbook of Fluid Dynamics," Sect. 17, McGraw-Hill, New York (1961).

Manuscript received November 5, 1962; revision received August 5, 1963; paper accepted August 8, 1963. Paper presented at A.I.Ch.E. New Orleans meeting.

Single-Particle Studies of Ion Exchange in Packed Beds: Cupric Ion-Sodium Ion System

M. GOPALA RAO and M. M. DAVID
University of Washington, Seattle, Washington

Considerable work has been expended on the development of analytical methods for predicting the performance of ion-exchange materials in packed beds. The resulting methods however have had only limited utility for design purposes because the physical and mathematical complications of the problem have necessitated use of various simplifying assumptions which have restricted the general applicability of the methods. Numerical techniques with high-speed computers offer a potential means for handling the mathematical complications of packed-bed systems without resort to undue simplifying assumptions. To use these techniques though, adequate models for the process and values for the rate constants included in these models must be available. These requirements demand in turn an extensive body of data for ion exchange in packed beds, both to verify proposed or suggest new models and to obtain generalized correlations for the rate constants in the models. The present study was undertaken to supply such data by an intensive investigation over a wide range of operating conditions of the exchange rate of copper ions for sodium ions on a typical cation exchanger, Dowex 50W-X8. Choice of this system was based on the relative sparsity of comprehensive rate data for the exchange of ions with unequal valences (especially in concentrated solutions), the extensive equilibrium data available for the system (*23*), the suitability of the system for the experimental procedure, and industrial interest in the system (*23*). Ion exchange of copper for sodium has been studied in dilute solutions by Selke and Bliss (*21*), but extensive rate studies of this system are lacking.

CURRENT CONCEPTS

Although ion exchange is essentially a metathical process which for the reaction of this study can be written as $Cu_r + 2Na_s \rightleftarrows Cu_s + 2Na_r$ (r and s denote the exchanger and external solution phases, respectively), the rates of ion exchange are determined by the mass transfer steps in the process. For the modern ion exchangers which are usually produced as small porous particles, the overall rate of exchange is controlled either by the resistance to mass transfer between the external fluid and the exchanger surface, by the resistance to mass transfer within the particle, or by the combination of these two resistances. As in other interphase transfer processes equilibrium is considered to exist between the two phases at the boundary formed by the exterior surface of the particle.

In packed beds of ion-exchange materials mass transfer from the bulk solution to the exchanger surface is effected by both convection and ionic diffusion. The rate of mass transfer for this step has usually been described in design

---

M. Gopala Rao is at Gonzaga University, Spokane, Washington.

methods (for example *5, 19, 20, 21, 25*) by an equation of the type

$$\frac{dq}{dt} = k_L\, s\, (c - \bar{c}) \qquad (1)$$

and various packed-bed *j*-factor relationships have been used to correlate the mass transfer coefficient, k_L (for example *2, 20*). For the usual case where the exchanging ions have different self-diffusivities, theoretical studies (*18*) indicate that the use of Equation (1) would be complicated by variation during the exchange process of both the total solution normality at the interface and the effective diffusivities, and consequently the mass transfer coefficients, of the exchanging ions. A mathematical analysis embodying these effects is available only for exchange of ions of equal valence, linear equilibrium, and consideration of the transfer process as strictly ionic diffusion across a stagnant film (*18*); it would appear that this analysis does not adequately allow for eddy convection effects. In a recent study (*7*) Equation (1) was found as successful for correlating the rate data for uni-univalent exchange as the more complicated relationship including the changes in interface-solution concentration and ion diffusivities.

Mass transfer within the exchanger is also a diffusional process. In design equations the internal diffusional process has usually been represented by Fick's second law or simplifications thereof, with a constant value of the internal diffusivity for a given ionic system (for example *5, 20, 25*). This approach has also been used to correlate experimental data on internal diffusion rates in packed beds (for example *20, 26*). However theoretical considerations as well as recent experimental work show that for the exchange of ions with different internal self-diffusivities the resulting electric field produces a diffusion coefficient (as defined by Fick's law) which is a function not only of the exchanging ions but also of exchanger composition (*10, 11, 16*). Integration of Fick's second law including the variable diffusion coefficient has presently been done only for equal-valent and uni-divalent exchange, with the exchanger initially containing only one ionic species, the exchanger surface always saturated with the entering species, negligible anion content of pore solution, and no change in exchanger volume (*11, 16*). For cases where both the internal and external resistances to mass transfer are important the presently available design techniques are limited to rate equations in which the external mass transfer coefficient and the internal diffusion coefficient are both constant, and change in normality of the interface solution is neglected (for example *17, 20, 25*).

EXPERIMENTAL

The single-particle method described by Gopala Rao (3) and Kuo (14) was developed and used in the present study. In this method a single spherical ion-exchange particle charged with an ion containing a radioactive tracer is placed in a small bed of similarly sized glass beads, and a solution of known composition is passed through the bed at a controlled flow rate. The amount of exchange occurring is so small that the solution composition remains essentially constant, and the rate of exchange is determined by continuously monitoring the amount of radioactive tracer ion present in the ion-exchange particle. Measurement of the particle diameter permits determination of the surface area for mass transfer between the solution and solid phases. The single-particle method provides a more direct and much less difficult way to determine ion-exchange rates and the effects of operating variables thereon than the often used deep-bed method and avoids or minimizes various complicating factors encountered with concentrated solutions in differential beds.

The ion exchanger used in the study was Dowex 50W-X8, a typical modern cation exchanger available in the form of small spheres. This exchanger contains nuclear sulfonic-acid exchange groups distributed uniformly throughout a structure of polystyrene cross-linked with divinyl benzene. A small batch of the exchanger was pretreated by several conversions alternately to the copper and sodium forms, and individual particles were selected for sphericity and freedom from flaws by examination with a microscope. The diameters of the particles used in the study were measured either by using a stage micrometer and camera lucidas with the microscope or with a micrometer eyepiece. Three particles of 1.09-mm. diameter (Na form) were used throughout the rate studies, except for some preliminary runs which are included in Figure 3.

The bed used in the rate studies was approximately 4 cm. high and 1 sq. cm. in cross section, with the ion-exchange particle located approximately 1 cm. from the bottom and on the vertical axis of the bed. The bed was supported by a fritted-glass disk sintered to the walls of the glass tube containing the bed, and a plug of glass wool at the top of the bed was used to maintain the bed in position and serve as a distributor. The ion-exchange particle when placed in the bed was in sodium form, with sodium-22 present as a tracer. Care was taken to maintain the bed and feed lines full of liquid during assembly of the apparatus, to prevent the introduction of air bubbles into the system. The apparatus was so constructed that by quickly turning a large-bore three-way stopcock a predetermined flow rate of solution through the bed could be started almost instantaneously. The flow rate was also checked throughout the run by measurements of the effluent rate. Almost all runs were made downflow. The radioactivity of the particle in the bed was measured by a Geiger-Mueller probe-ratemeter-recorder train. The ratemeter used had a time constant of 12 sec.

Prior to the start of a run the radioactivity of the particle in position in the bed was measured for approximately 10 min., with distilled water passing through the bed. Copper chloride solution was then admitted to the bed at the desired flow rate, and the residual radioactivity of the particle was continuously recorded as a function of time. The background count was measured both before and after the run. Following the run the particle was removed from the bed and reconverted to the sodium form. Because of the low time constant for the ratemeter the output data for a run were in the form of a somewhat wiggly curve, which could easily be averaged by eye to give the residual sodium content of the particle to within 2% of the initial value. The smoothed data were corrected for background count and were replotted in terms of copper content of the exchanger, for treatment as discussed below.

During the course of the work results were published (*12*) for an ion-exchange equilibrium study which found that individual particles of an ion exchanger similar to that used in the present study were not homogeneous in ion-exchange properties. The capacities and equilibrium characteristics in 0.1 N and 1.0 N solutions were therefore measured for the particles used in the rate studies, as well as for several other particles ranging from 0.83 to 1.24 mm. in diameter. The procedure used essentially was to permit the particle charged with tagged sodium to equilibrate with an accurately measured small volume (0.25 to 1.0 ml.) of solution containing known concentrations of sodium and copper ions. The amount of exchange

TABLE 1. PROPERTIES OF THE PARTICLES

Particle	Particle diameter, mm.* NaR in water	CuR₂ in water	Sodium† capacity of particle meq.	Exchange capacity meq./ml. of Na form of resin
A	1.09	1.07	1.409	2.07
B	1.07	1.10	1.421	2.24
C	1.03	1.01	1.291	2.24
G	1.24	1.25	2.180	2.21
H	0.86	0.81	0.725	2.15
J	0.83	0.80	0.688	2.27

* Average of diameter values at three different orientations.
† Pore solution excluded.

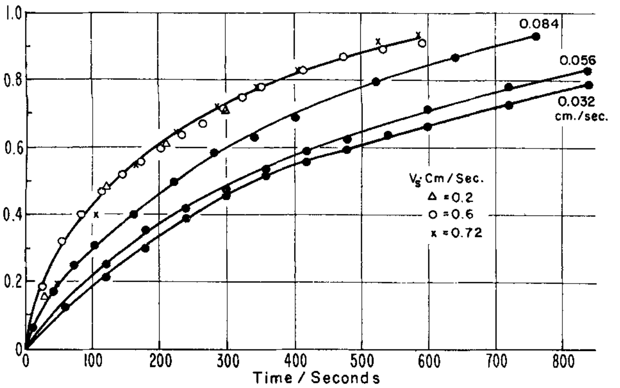

Fig. 1. Experimental curves for 0.1 N cupric chloride solution.

occurring was negligible compared with the ionic content of the solution, and knowledge of the radioactivity of the particle before and after equilibration permitted calculation of the equilibrium composition of the exchanger phase. The particles all showed very good agreement of specific capacity and excellent agreement of equilibrium compositions, both from particle to particle and with published data for the system cupric ion-sodium ion-Dowex 50 (*23*). Other work (*4*, *13*, *14*) also substantiates the uniformity of Dowex 50W exchanger. Characteristics of the particles used in the equilibrium studies are given in Table 1.[*]

Limitations of Study

The factors important in determining the rates of ion exchange in a packed bed for a given system include the exchanger particle size and cross linkage, the solution concentration and composition, the flow rate through the bed, and the temperature. The present study was chiefly concerned with the effects of solution concentration and flow rate. The study used only Dowex 50W particles with 8% cross linkage and diameters of 1.09 mm. (sodium form). All runs were at room temperature (approximately 23°C.). Copper chloride solutions of 0.01 N, 0.1 N, 1.0 N, 2.0 N, and 4.0 N were employed. One run was also made with a 1.0 N sodium chloride feed solution to measure the self-diffusivity of sodium inside the exchanger. The range of flow rates used varied with the solution concentration, as discussed below, but the overall range of flow rates covered in the study included superficial velocities from 0.02 to 3 cm./sec. The equilibrium studies were restricted to 0.1 N and 1.0 N solutions, since the results obtained for these concentrations were in excellent agreement with the data of Subba Rao (*23*).

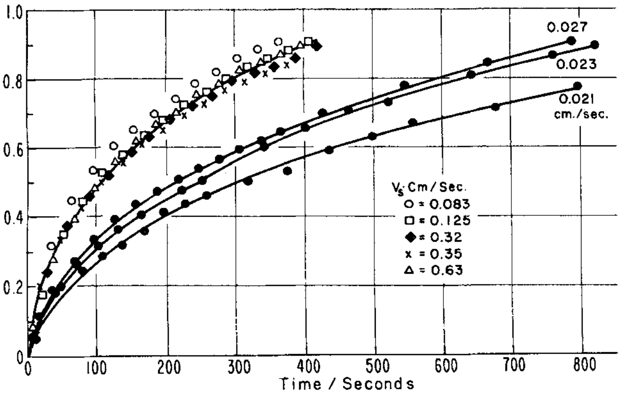

Fig. 2. Experimental curves for 1.0 N cupric chloride solution.

RESULTS AND DISCUSSION

Typical experimental results for the rate studies are given in Figures 1 and 2 where data for the runs with 0.1 N and 1.0 N solutions are presented as plots of $(q/a)_{\mathrm{Cu}}$, the fraction of exchange capacity in the copper form, vs. time, with the superficial velocity of solution through the bed as the curve parameter.[*] Experimental data points for the 0.01 N, 2 N, and 4 N studies are included in Figures 4, 5, and 6. Though the data for the latter portions of long duration runs are not included in the figures, all runs were continued to a $(q/a)_{\mathrm{Cu}}$ of approximately 0.9.

At each concentration studied an attempt was made to vary flow rate from velocities sufficiently high that fluid velocity no longer affected exchange rate to flow rates sufficiently low that mass transfer between the bulk liquid and exchanger surface controlled the exchange rate for at least a portion of the run. However it was not found possible to reach the velocity-independent state with 0.01 N solutions, and as discussed below even with the very lowest flow rates practical with the apparatus (0.02 to 0.03 cm./sec.) a completely liquid-film controlled situation could not be obtained with solution concentrations greater than 0.1 N. As may be noted from the figures flow rate did influence the exchange rate at all concentrations for sufficiently low velocities, thus showing that the resistance to mass transfer through the liquid film was important in determining the rate of exchange for such cases.

Liquid-Film Mass Transfer Coefficients for Dilute Solutions

Dilute solutions and an equilibrium favorable to the entering ion promote control of the exchange rate by the liquid film (*1*, *9*). For 0.01 N solution, the equilibrium is almost irreversibly in favor of the copper form of the exchanger until the exchanger is practically saturated with copper (*23*). For this type of equilibrium situation and an external solution containing only copper, if the liquid-film resistance is rate controlling, Equation (1) becomes (*14*)

$$\frac{d(q/a)_{\mathrm{Cu}}}{dt} = \frac{k_L\, s}{a} C_o \qquad (2)$$

In accordance with Equation (2) a plot of $(q/a)_{\mathrm{Cu}}$ vs. time should be linear, and in Figure 4 the first portions of the curves, in marked contrast to the curves for higher concentrations, are straight lines. As copper content of the particle increases, the internal-diffusion step also becomes important as a rate-determining factor, and the experimental curves in Figure 4 deviate from linearity. Mass transfer coefficients were calculated for the data of Figure 4 by use of Equation (2), and the results are presented in Figure 3 on the *j*-factor correlation plot for fixed beds proposed by Carberry (*2*). Also included in Figure 3 are results obtained from preliminary 0.01 N runs with a 1.16-mm. diameter particle of Dowex 50-X8 exchanger.

In principle mass transfer coefficients for less favorable equilibria can be evaluated by defining an overall mass transfer coefficient by

$$\frac{d(q/a)}{dt} = \frac{K_L\, s\, C_o}{a} (1 - c^*/C_o) \qquad (3)$$

where c^*/C_o is in equilibrium with (q/a), K_L is evaluated as a function of time by using slopes of the (q/a) vs. time curves, and by extrapolating to zero time (*20*). The

---

[*] The capacity values reported in Table 1 for the particles used in the rate studies were rechecked during the course of the work. However subsequent investigations (*14*) report capacities of Dowex 50W-X8 approximately 25 to 30% higher than indicated in Table 1. The only results presented here which are affected by the capacity value are the k_L's which are directly proportional to capacity. All other calculations are based on ratios and are independent of the actual value of the capacity.

[*] A complete tabulation of experimental results and further details on apparatus, experimental procedures, and calculational methods are given in reference 8.

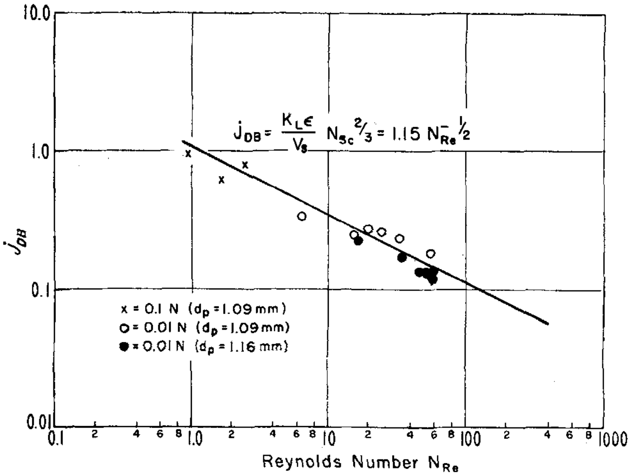

Fig. 3. *j*-factor correlation of liquid-film coefficients for 0.01 N 0.1 N cases.

k_L values for the 0.1 N runs in which the equilibrium was also very favorable to the copper form were obtained in this fashion and are plotted in Figure 3. Both the 0.01 N and 0.1 N data appear to conform to the type of *j*-factor correlation given in Figure 3. The k_L values for higher concentrations could not be obtained by Equation (3) with any precision and showed considerable deviation from the *j*-factor correlation.

In preparing Figure 3 the density and viscosity of the 0.01 N and 0.1 N solutions were taken as those of pure water, ϵ as 0.4, and Ds as the diffusivity of the copper ion at infinite dilution $(0.72)(10^{-5})$ sq. cm./sec. Use of a counterdiffusion coefficient as calculated by the methods proposed by Gilliland et al. (*6*) instead of the self-diffusivity would lower all the experimental points by approximately 15%.

Interpretation of the Internal-Diffusion Controlled Results

For the uppermost curves in Figures 1, 2, 5, and 6 the fluid velocity through the bed no longer influences the rate of ion exchange, and the rate is therefore completely internal-diffusion controlled. A similar curve was obtained early in the study for 0.01 N solutions at moderately high velocities. This curve was considerably lower than the corresponding curves at higher concentrations, and subsequent investigation indicated that the apparent internal-diffusion controlled curve actually resulted from bypassing effects in the bed at the higher fluid velocities. Later 0.01 N runs at similarly high velocities, made upflow and with care to avoid channeling effects, had properly higher exchange rates and k_L values in agreement with the *j*-factor correlation. Fluid velocities at least two orders of magnitude higher than those used in the present study would apparently be needed to approach, if possible, internal-diffusion control at 0.01 N concentration for the system and particle size of the study.

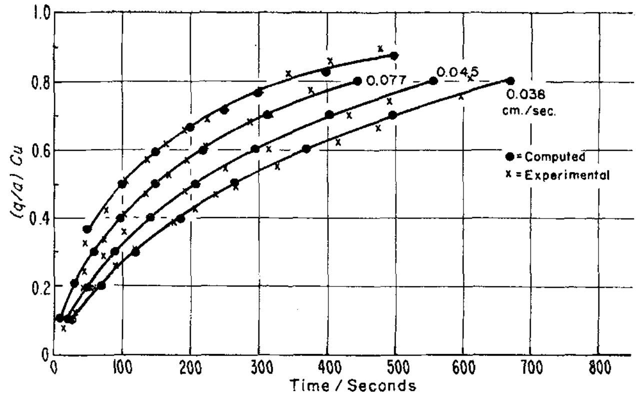

Fig. 5. Experimental and predicted curves for 2.0 N solutions. For uppermost curve v_S = 0.32 to 0.52 cm./sec.

The experimental results in the range of internal-diffusion control were interpreted by both constant diffusivity and variable diffusivity methods. For the former method use was made of the very satisfactory approximation of Vermeulen (*27*) for the exact series solution of Fick's second law with the boundary condition of exchanger surface saturated with the incoming ion

$$(q/a)_{Cu} = \left[1 - \exp\left(\frac{-\pi^2 (Ds)_{AB}\, t}{r_o^2} \right) \right]^{1/2} \qquad (4)$$

where $(Ds)_{AB}$ is the value of internal diffusivity for ion B replacing ion A and r_o is the radius of the particle. $(Ds)_{AB}$ values computed from Equation (4) tended to increase with q/a, but back calculation of the internal-diffusion exchange curves by use of the average value of $(Ds)_{AB}$ for the q/a range of 0.5 to 0.9 (where Ds was fairly constant) resulted in a acceptably good match with the experimental curves. The average $(Ds)_{AB}$ values thus obtained are given in Table 2 and are seen to vary relatively little with solution concentration. A solid-diffusion controlled run was also made with a 1.0 N sodium chloride solution to determine the self-diffusivity of the sodium ion in Dowex 50W-X8 exchanger, and this run is also included in Table 2.

Interpretation of the experimental data by the variable diffusivity model was made by use of the explicit approximative expression provided by Plesset et al. (*16*) for representing the results of their numerical intergration of Fick's second law with a variable interdiffusivity coefficient. For bivalent-monovalent exchange the variable diffusivity is given by (*16*)

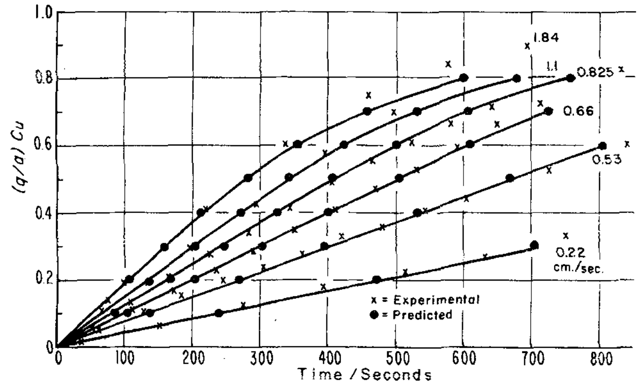

Fig. 4. Experimental and predicted curves for 0.01 N solution.

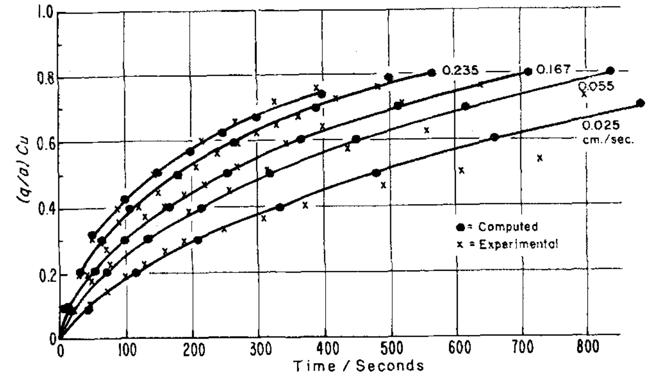

Fig. 6. Experimental and predicted curves for 4.0 N solution. For uppermost curve v_S = 0.30 to 0.35 cm./sec.

TABLE 2. EXPERIMENTAL VALUES OF INTERNAL DIFFUSIVITIES

Solution Concentration	Constant interdiffusivity $(D_S)_{AB}$ 10^{-6} sq. cm./sec.	Self-diffusivity ratio α (D_{SA}/D_{SB})
0.1 N	0.74	10
1.0 N	0.90	6
2.0 N	0.90	6
4.0 N	0.65	13
1.0 N NaCl	1.6 (self-diffusivity of sodium)	

$$(D_S)_{AB} = \frac{D_{SA}\,(1 + q/a)}{(D_{SA}/D_{SB})\,(1 - q/a) + 2q/a} \qquad (5)$$

D_{SA} and D_{SB} are the self-diffusivities in the exchanger of the leaving and entering ions respectively (sodium and copper, respectively, in the present study), and q/a is the fraction of the exchanger capacity in the form of the entering divalent ion at the point where $(D_S)_{AB}$ is being determined. Equation (5) is obtained by applying the Nernst-Planck equation to the counterdiffusion of ions inside the exchanger under conditions of electro-neutrality and no electrical current. Integration of Fick's second law incorporating Equation (5) was accomplished by assuming no pore solution, constant exchanger diameter, invariant self-diffusivities, the exchanger initially in the *A* form entirely, and the exchanger outer surface saturated with *B* for all time greater than zero (*16*). Insofar as possible the solid-diffusion data of the present study conformed to these requirements.

The equation suggested by Plesset et al. is

$$(q/a)_{Cu} = \{1 - \exp[\pi^2(f_1(\alpha)\tau + f_2(\alpha)\tau^2 + f_3(\alpha)\tau^3)]\}^{1/2} \qquad (6)$$

where α is the self-diffusivity ratio D_{SA}/D_{SB}, τ is $\frac{D_{SA}\,t}{r_o^2}$, and the f's are empirical functions of α. For values of τ much less than 1, as were encountered in the present study, Equation (6) becomes

$$(q/a)_{Cu} = \{1 - \exp\,[\pi^2 f_1(\alpha)\;\tau]\}^{1/2} \qquad (7)$$

where f_1 is given by $1/f_1 = -\,0.64 - 0.36\alpha^{0.668}$ for $1 \leq \alpha \leq 20$. Equation (7) was used to calculate average values of α for the internal-diffusion controlled data by trial and error, with the results shown in Table 2. The experimentally-determined value of D_{SA} for 1.0 N solutions and a particle diameter of 1.09 mm. were used for all calculations of α.

The variation in α reported in Table 2 may actually reflect to some extent a variation of the self-diffusivity ratio with concentration. Part of the variation however is undoubtedly due to some of the values used in the calculation of α and to discrepancies between experimental conditions and the conditions assumed by Plesset et al. in their derivation. Evidence in the literature indicates that D_{SA} may vary with concentration of the external solution (9, 24), as may the particle radius (9, 14). It is also probable that D_{SA} varies as a function of the exchanger composition (22). Additionally chloride ion will be present in the exchanger pores under equilibrium conditions and amounts to approximately 15% of the exchanger capacity for the 4.0 N solutions (23). Since no chloride ion is present in the pores at the start of a run, copper and chloride ions from the external solution, and probably some of the replaced sodium ions as well, will tend to diffuse into the exchanger particle. The net effect of this pore solution diffusion will probably be to lower the experimental rate curve and thereby result in a larger value for α. This effect would be most noticeable with the 4 N solution and may account for the unusually high value of α for this case. Exact corrections for all the effects listed above would be diffcult, even if the necessary data were available.

Use of the average values of α given in Table 2 to calculate theoretical particle saturation curves resulted in acceptable matching of the experimental curves, as shown by the uppermost curve in Figures 5 and 6. A discrepancy between the calculated and experimental curves not readily shown on these figures but noted also for the constant-diffusivity model comparisons is a perceptibly larger initial slope for the theoretical curves during the very first portion of the curve. This indicates that at the very first of the run the liquid film is of some importance in determining the rate of exchange, even for situations which appear to be completely internal-diffusion controlled.

Comparison of Equations (4) and (7) indicates why much of the past data for internal diffusion in ion exchangers could be correlated successfully with a constant value of the internal diffusivity, even though it is now well established that the interdiffusivity coefficient varies with exchanger composition. For initial and boundary conditions of the particle initially saturated with one ion and the surface maintained saturated with the other ion during the exchange process, and τ small compared with 1

$$-\,(D_S)_{AB} = f_1(\alpha)D_{SA} \qquad (8)$$

If the internal self-diffusivities of the exchanging ions are taken as constant, as they must to use Equation (6), the right side of Equation (8) is a constant. The value of the interdiffusivity coefficient will of course differ for the two directions of exchange. With the α and D_{SA} values for 1 N solutions given in Table 2, $(D_S)_{AB}$ is computed as (0.88) (10^{-6}) sq. cm./sec., which compares well with the experimental value of (0.90) (10^{-6}) sq. cm./sec. A good concordance between calculated and experimental values of $(D_S)_{AB}$ has also been noted for the barium-sodium system, for both directions of exchange (*14*). It appears likely that for many cases where internal diffusion controls the rate and for which the above-listed initial and boundary conditions are applicable, the use of a single value for the internal diffusivity is adequate to represent the exchange process. For these cases the value of the interdiffusivity coefficient can be calculated from equations similar to Equation (8) (9), if the self-diffusivities for the exchanging ions are known.

Equations (4) and (6) can also be used together to calculate an integral interdiffusivity coefficient appropriate for a given value of q/a. The interdiffusivity coefficient thus computed will increase as q/a increases and will be somewhat larger than predicted by Equation (8) from known values of D_{SA} and D_{SB}. The experimentally determined values of $(D_S)_{AB}$, as noted earlier, did tend to increase with q/a, as the variable-diffusivity model predicts. The use of Equation (7) rather than Equation (6) to interpret the experimental data probably accounts for the experimental points on the internal diffusion curve of Figures 5 and 6 being slightly above the predicted values at the upper end of the curve. If the change in interdiffusivity coefficient with q/a is appreciable (if τ is not small compared with 1), the variable-diffusivity model should provide a better fit of data than will the constant diffusivity model.

Intermediate Cases

For most of the runs in the present study both internal and liquid-film resistances to mass transfer were important in determining the exchange rate during a major portion of the run. For such cases exact solutions relating q/a to *t* are not available if the equilibrium at the interface is highly nonlinear, as for the copper-sodium system. Accordingly resort was made to numerical methods programmed for computer solution to compute theoretical particle-saturation curves which could be matched with the experimental curves to permit evaluation of pertinent rate constants.

Finite-difference forms of Equation (1) and Fick's second law were used to establish the equations for the numerical computations. The equilibrium data of Subba Rao (*23*), expressed in polynomial form with a separate expression for each concentration, were used for the interface equilibria. The equation forms and methods of solution are almost identical with those used for unsteady state heat transfer by conduction in a sphere when heat transfer to the outer surface of the sphere is by convection (*15*), except that the interface compositions in the two phases are not equal but rather are related by equilibrium requirements. Material balances for a small time increment are written for the outer surface of the spherical particle and for thin concentric spherical shells of equal thickness within the particle.* Ten or more such shells were used in all computations. The material balance equations for inside the particle are essentially the same as those of Helfferich and co-workers (*11, 16*). In the computations k_L was considered to be constant throughout a run, and the solution normality at the interface was taken as the bulk solution normality. For higher concentrations the exchanger capacity was corrected to include pore solution by the data of Subba Rao. The initial computer program (*28*) was based on a constant value for the internal diffusivity and was checked by using the program to compute known solutions for the case of a linear isotherm. In working with this program the value of $(D_S)_{AB}$ for the concentration being studied, given in Table 2, was used, and the value of k_L was varied to try to obtain a good match of experimental and predicted curves. Values of k_L indicated by the initial slopes of the experimental curves were used to aid in the initial choice of proper values for the mass transfer coefficient. However except for the 0.01 N cases and a few other scattered runs, adequate matching of the experimental and computed curves could not be obtained. The program was then modified to include a variable diffusivity, defined by Equation (5), for each shell in the exchanger (*28*). The computations for inside the exchanger then became essentially those used by Plesset et al., and the new program was verified by duplicating some of the curves furnished by Plesset. Values of α proper to the concentration being studied, as given in Table 2, were used, and for the 0.01 N and 0.1 N cases values of k_L determined experimentally (Figure 3) were employed. For higher concentrations the initial slope of the experimental curves was again used to aid in the initial choice of k_L, but the value of k_L was varied to obtain the best possible curve match. Computations were performed with an IBM-709 computer. Several minutes computing time was frequently necessary to obtain a single trial curve because of the extremely small time increments which had to be employed to insure stability of the solution.

A comparison of computed and experimental curves is given in Figures 4, 5, and 6. Figures 4 and 6 are included because the uppermost curve on the former and the lowermost curve on the latter are the poorest matches obtained. Figure 5 is more representative of the sort of curve matching found, and in general use of the variable-diffusivity model was relatively successful for matching the theoretical curves. That the variable-diffusivity model was satisfactory for curve matching in intermediate cases and the constant diffusivity model was not indicates that the equivalence of these two models found for the internal-diffusion controlled case is not extensible to other boundary conditions.

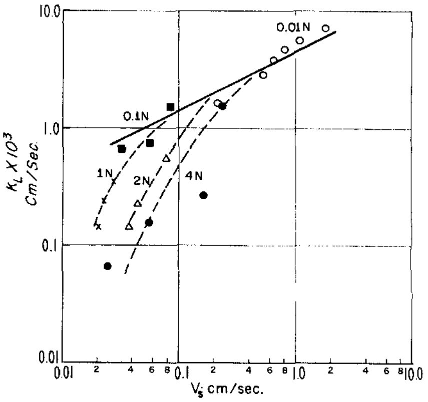

Fig. 7. Liquid-film coefficients from curve matching.

The k_L values used for the curve-matching process are shown in Figure 7 as a function of fluid velocity and solution concentration. The k_L values for the 0.01 N and 0.1 N cases are, as noted above, experimentally determined values and show the effect of velocity predicted by the *j*-factor correlation. The k_L values for higher concentrations, determined by curve matching, all are lower than the k_L vs. v_s line defined by the 0.01 N and 0.1 N cases and show a much greater influence of fluid velocity. Lower values of k_L at higher concentrations would be expected because of both the lower values of ionic diffusivities at higher concentrations and the effect of pore solution, discussed above, in producing lower experimental curves. The electric field effects resulting from countertransfer of ions with different self-diffusivities may also be partly responsible for the lower k_L values at higher concentrations. Theoretical considerations (*18*) indicate that for copper replacing sodium k_L should be lower at the start of exchange, and it is the early part of the particle saturation curve which is most important in determining the value of k_L by curve matching. In addition to the above factors the use of k_L, in effect, as a correction factor to compensate for the defects discussed earlier of the variable-diffusivity model may also influence the k_L values obtained.

Inadequate data prevent quantitative evaluation of the effects of the above factors on k_L, but it should be noted that all the factors discussed are primarily concentration-dependent effects. The apparent influence of velocity on k_L at the higher concentrations is difficult to explain satisfactorily, and it is difficult to say if the trends shown are genuine effects or result from defects in the interpretive model used.

CONCLUSIONS

In the present study for dilute solutions (0.01 N and 0.1 N) the rate of mass transfer from the bulk solution to the particle surface can be represented adequately by Equation (1), by using a constant value of mass transfer coefficient at a given flow rate and by neglecting changes in the interface solution normality. This is true both for operating conditions such that the liquid film controls the rate entirely and for conditions such that both liquid-film and internal resistances are important; the mass transfer coefficients can be correlated by generalized *j*-factor relationships for packed beds. These results and similar finding in other comparable packed-bed studies of ion ex-

---

* Further details on the equations used are available in references *8* and *27*.

change with dilute solutions and equilibrium favorable to the entering ion (*14, 20*) vindicate the widespread use of Equation (*1*) for representing the rate of exchange between bulk solution and exchanger surface for the case of dilute solutions and favorable equilibria.

The experimental data for internal-diffusion control of exchange rate could be correlated by use of Fick's second law with either a constant internal diffusivity or a more theoretically correct variable interdiffusivity coefficient. The variable interdiffusivity coefficient includes effects of the electric field resulting from counterdiffusion of ions possessing different internal self-diffusivities. Use of the variable diffusivity was necessary to obtain a mathematical model for predicting exchange curves which matched reasonably well the experimental curves at higher concentrations where both liquid-film and internal diffusion were important in determining the rate of exchange. Comparison of the correlating equations used for the strictly internal-diffusion controlled case shows that a constant internal diffusivity will often be adequate if the exchanger is initially saturated with one ion and the surface is maintained saturated with the entering ion during the exchange process. That the use of a constant interdiffusivity value is not valid for other types of boundary conditions however is indicated by the need to use the variable interdiffusivity for intermediate cases. For those cases in which the constant interdiffusivity is satisfactory, its value can frequently be computed from the internal self-diffusivities of the exchanging ions.

For concentrated solutions the values of the liquid-film mass transfer coefficients obtained by curve matching could not be correlated with similar coefficients for dilute solutions. While this situation is undoubtedly caused in part by effects to be expected with concentrated solutions, some of the difficulty may stem from the use of a liquid-film model which neglects the effects produced by the counterdiffusion of ions with different self-diffusivities. Further work in this area is necessary before ion-exchange rates in concentrated solutions can be predicted when the liquid film is an important factor in determining the rate.

ACKNOWLEDGMENT

The authors express their appreciation to the Engineering Experiment Station at the University of Washington and to the National Science Foundation for financial support during the investigation.

NOTATION

a = exchange capacity, meq./unit quantity of exchanger
c = concentration of ion in bulk solution, meq./ml.
$\bar{c}$ = concentration of an ion in the interface solution immediately adjacent to exchanger particle, meq./ml.
c_o = total solution normality, meq./ml.
c^* = concentration of an ion in equilibrium with exchanger of composition q/a, for a total solution normality c_o, meq./ml.
d_p = particle diameter, cm. (except where otherwise noted)
D_B = diffusivity of ion B in the Schmidt number used for correlating the external mass transfer coefficients, sq. cm./sec.
D_{SA} = self-diffusivity of ion A inside the exchanger, sq. cm./sec.
D_{SB} = self-diffusivity of ion B inside the exchanger, sq. cm./sec.
$(D_S)_{AB}$ = mutual internal-diffusion coefficient for ion B replacing ion A, sq. cm./sec.
k_L = external mass transfer coefficient, cm./sec.
K_L = overall external mass transfer coefficient defined by Equation (3), cm./sec.
N_{Re} = Reynolds number for packed beds = $d_p v_s \rho_L / \mu_L \epsilon$
N_{Sc} = Schmidt number
q = exchanger composition, meq. of a given ion per unit quantity of exchanger
r_o = radius of exchanger particle
s = external surface area of exchange, sq. cm./prescribed quantity of exchanger
t = time
v_s = superficial velocity in bed, cm./sec.

Greek Letters

α = ratio of internal self-diffusivities, D_{SA}/D_{SB}
ϵ = void fraction of bed
ρ_L = liquid density, g./cc.
τ = dimensionless time-factor group, $D_{SA}t/r_o^2$
μ_L = liquid viscosity, poise

LITERATURE CITED

1. Boyd, G. E., A. W. Adamson, and L. S. Meyers, Jr., *J. Am. Chem. Soc.*, **69**, 2836 (1947).
2. Carberry, J. J., *A.I.Ch.E. Journal*, **6**, 460 (1960).
3. David, M. M., and M. Gopala Rao, *Chem. Age of India*, **12**, No. 4, p. 297 (1961).
4. Eatough, N., M.S. thesis, Univ. Wash., Seattle, Washington, (1960).
5. Gilliland, E. R., and R. F. Baddour, *Ind. Eng. Chem.*, **45**, 330 (1953).
6. ——————, and D. J. Goldstein, *Can. J. of Chem. Eng.*, **35**, 10 (1957).
7. Glaski, F. J., and J. S. Dranoff, *A.I.Ch.E. Journal*, **9**, 426 (1963).
8. Gopala Rao, M., Ph.D. thesis, Univ. Wash., Seattle, Washington (1962).
9. Helfferich, F., "Ion Exchange," McGraw-Hill, New York (1962).
10. ———, *J. Phys. Chem.*, **66**, 39 (1962).
11. ———, and M. S. Plesset, *J. Chem. Phys.*, **28**, 418-24 (1958).
12. Hogfeldt, E., *Arkiv. Kemi.*, **13**, 491 (1959).
13. Iungerich, C., M.S. thesis, Univ. Wash., Seattle, Washington (1961).
14. Kuo, J. C. W., and M. M. David, *A.I.Ch.E. Journal*, **9**, 365 (1963).
15. Mickley, H. F., T. K. Sherwood, and C. E. Reed, "Applied Mathematics in Chemical Engineering," 2 ed., McGraw-Hill, New York (1957).
16. Plesset, M. S., F. Helfferich, and J. N. Franklin, *J. Chem. Phys.*, **29**, 1064-69 (1958).
17. Rosen, J. B., *Ind. Eng. Chem.*, **46**, 1590 (1954).
18. Schlogl, R., and F. Helfferich, *J. Chem. Phys.*, **26**, 5-7 (1957).
19. Selke, W. A., in "Ion Exchange Technology," Nachod, F. C., and J. Schubert, ed., Academic Press, New York (1956).
20. Selke, W. A., Y. Bard, A. D. Pasternak, and S. K. Aditya, *A.I.Ch.E. Journal*, **2**, 468 (1956).
21. Selke, W. A., and H. Bliss, *Chem. Eng. Progr.*, **47**, 529 (1951).
22. Soldano, B. A., and G. E. Boyd, *J. Am. Chem. Soc.*, **75**, 6107 (1953).
23. Subba Rao, H. C., and M. M. David, *A.I.Ch.E. Journal*, **3**, 187 (1957).
24. Tetenbaum, M., and H. P. Gregor, *J. Phys. Chem.*, **58**, 1156 (1954).
25. Tien, Chi, and George Thodos, *A.I.Ch.E. Journal*, **5**, 373 (1959).
26. Vasishth, R. C., and M. M. David, *ibid.*, p. 391.
27. Vermeulen, Theodore, *Ind. Eng. Chem.*, **45**, 1664 (1953).
28. Von Fuchs, G., M.S. thesis, in preparation, Univ. Wash., Seattle, Washington (1962).

Manuscript received March 26, 1963; revision received July 17, 1963; paper accepted July 23, 1963. Paper presented at A.I.Ch.E. New Orleans meeting.